RESEARCH MEMORANDUM

EXPERIMENTAL INVESTIGATION OF THE MIXING LOSS BEHIND THE TRAILING EDGE OF A CASCADE OF THREE 90° SUPERSONIC TURNING PASSAGES

By Luke L. Liccini

Langley Aeronautical Laboratory
Langley Air Force Base, Va.

NATIONAL ADVISORY COMMITTEE
FOR AERONAUTICS

WASHINGTON

August 15, 1950

NACA RM L50F21a

NATIONAL ADVISORY COMMITTEE FOR AERONAUTICS

RESEARCH MEMORANDUM

EXPERIMENTAL INVESTIGATION OF THE MIXING LOSS BEHIND THE TRAILING EDGE OF A CASCADE OF THREE 90° SUPERSONIC TURNING PASSAGES

By Luke L. Liccini

SUMMARY

A two-dimensional cascade of three 90° turning passages, designed by the method of characteristics, was tested at an inlet Mach number of 1.81. The total loss across the cascade was 9 percent. Of this total, approximately 5 percent is chargeable to the mixing process downstream of the trailing edges. Although a variation of the boundary-layer thickness occurred across the span and resulted in a nonuniform turning angle, the average turning was within 1° of the design value. The wake survey indicates that the velocity tends to become uniform very rapidly behind the trailing edge in the blade wake.

INTRODUCTION

Reference 1 presents several schemes of supersonic compressors, one of which would give high values of compression ratio if problems concerning efficient supersonic turning and diffusing in the rotor and stator design could be solved. For such a compressor, the stream enters relative to the rotor at a supersonic velocity and undergoes a large change of direction in the rotor. Leaving the rotor, the air then enters the stator at a high supersonic velocity and is diffused in the stator to subsonic velocity. A more detailed analysis of this type of compressor is presented in reference 2. The analysis in reference 2 shows that with a variable-geometry stator, a stage compression ratio of the order of 6 to 10 may be obtained with an adiabatic efficiency ranging from 75 to 80 percent, provided that a turning angle of the order of 90° can be accomplished in the rotor without large losses for an entrance Mach number of about 1.7. An experimental investigation was made (reference 3) of four 90° two-dimensional turning passages suitable for a compressor rotor at an inlet Mach number of 1.71. The measured losses varied from 5 to 15 percent of the inlet stagnation pressure. However, the results obtained in reference 3 do not include the mixing losses behind the trailing edges of the rotor blades.

The tests presented herin were made primarily to obtain an indication of the magnitude of the losses in the stagnation pressure due to the mixing phenomena behind the trailing edge of the best blade design given in reference 3. The mixing losses were evaluated from surveys made at 0.66 chord behind the trailing edge and inside the passage near the exit. The test Reynolds number was 5.08×10^6 based on the blade chord.

It should be noted that the problem of an efficient turn of this magnitude arises also in the design of turbines with relative supersonic entrance velocities.

SYMBOLS

A	cross-sectional area
c	blade chord
m	mass flow
p	static pressure
s	blade spacing
t	maximum thickness of blade
M	Mach number
P	stagnation pressure
T	static temperature, $^{\circ}F$ absolute
c/s	solidity
t/c	thickness ratio

Subscripts:

o	absolute inlet stagnation
1	entrance
2	exit
av	average
A	atmospheric

APPARATUS AND TEST METHODS

The design of the blade used in this investigation corresponds to model 3 in reference 3. The characteristics net and the theoretical local Mach number plotted against percent chord are presented in figure 1. The blade shape and the corresponding ordinates are presented in figure 2. The principal geometric parameters of the model used in this test and of model 3 of reference 3 are shown in table I.

The cascade tests were made in one of the blow-down jets of the Gas Dynamics Branch of the Langley Aeronautical Laboratory. The testing techniques used in this investigation were the same as those described in reference 3. The test section of the two-dimensional nozzle used in this investigation had a span of 3 inches and a height of 2.2 inches. The design of the nozzle was obtained from reference 3 and scaled directly to fit these tests with no consideration given to the difference in boundary layer, and, therefore, the test-section Mach number was 1.81 rather than 1.71. Figure 3 is a photograph of the test assembly with one side wall removed.

The model was constructed of metal and consisted of three turning passages formed by two blades and two blocks (fig. 4). One block formed a convex surface constructed to the ordinates of the blade's upper surface and the other formed a concave surface constructed to the ordinates of the blade's lower surface. Because the wake survey was made 2 inches behind the trailing edge, the outside walls were extended by a set of spacers to prevent any edge disturbances and, therefore, to prevent the flow from deviating far from the true wake direction (fig. 4). The blades were supported by pins (made integral with the blades) which extended through holes in the glass to a cantilever support attached to the side walls outside the glass. In this way, the pins exerted a minimum force upon the glass. The cantilever supports were so arranged that the center passage was as clear as possible for visual observations during the test. A photograph of a blade is shown in figure 5. As in reference 3, a "bleed-off" is provided at the entrance of the cascade to prevent the boundary layer at the top and bottom of the nozzle from entering the passages (fig. 4). The boundary layer along the side walls was not eliminated and, thus, entered the passages.

A wake survey 0.66 chord behind the trailing edge and a survey inside the center passage near the exit were made. The surveys of static pressures and pressures measured by total-head tube were made at three spanwise stations using a rake (fig. 6) which could be moved to any point in the wake. The positions of the surveys are shown in figure 4. The wake-survey position was chosen 2 inches behind the trailing edge because at this position it was estimated that no appreciable effects on the results due to limiting the cascade to three passages would exist, and

the mixing losses measured would be close to the true values. As is discussed subsequently in more detail, the results show that the choice of this position was very near to being correct. A conventional shadowgraph system was used to obtain photographs of the flow.

The method of calculation used in this investigation is the same as that used in reference 3 and is given in the appendix. The values of the average weighted exit Mach number and the average weighted stagnation-pressure recovery were calculated.

RESULTS AND DISCUSSION

Before the results obtained can be made applicable to an infinite cascade, it is necessary to analyze the effect of limitation of the number of passages considered. For the tests presented herein, three passages were represented. However, the flow behind the outside passages has on one side an actual blade wake, whereas on the other side a rigid wall is substituted for the direction of the blade wake. Therefore, the direction of the stream after the point corresponding to the trailing edge of the blade is fixed by the wall and not by the aerodynamic phenomena. The disturbances in the stream are reflected at the rigid walls and cross the wake in a different position than those of another blade of the cascade. In order to eliminate the wall effects, it is necessary that the walls have practically the same direction as the wake and that the disturbances reflected at the walls do not interfere with the survey.

Figure 7 is a schematic diagram of the flow disturbances behind the exit of the cascade obtained from the shadowgraph. This figure shows that the wake-survey position is located at the greatest distance behind the trailing edge which would still give results free from the reflected wall disturbances. If the survey were made at a distance greater than 2 inches, the wake survey of the center passage would include the effects of the disturbances reflected from the walls. The direction of the wake, as is discussed subsequently, is practically parallel to the direction of the wall; therefore, it can be concluded that the results obtained are the same as for an infinite cascade.

Figures 8 to 10 show the Mach number distribution at the three spanwise stations for the survey made inside the center passage as compared to the corresponding zones of the wake survey. The surveys made inside the passage indicate that the velocity near the convex surface tends to decrease to subsonic velocities. The wake survey indicates that the Mach number tends to become uniform in the blade wakes. The lowest Mach numbers occurred at the 32.5-percent-span station. Figure 11 shows a comparison of the static-pressure distribution at the three spanwise stations for the survey inside the passage with the corresponding zones of the

wake survey. The static-pressure distribution indicates that the velocity tends toward uniformity.

Figures 12 to 14 show the stagnation-pressure-recovery distribution for the survey made inside the center passage as compared to the corresponding zones of the wake survey. The surveys made inside the passages indicate that the major losses occur near the convex surface and, therefore, follow closely that indicated in reference 3. However, in the spanwise direction the major measured losses occur at the 32.5-percent-span station instead of at the 50-percent-span station. This indicates that the boundary-layer thickness is greater at the 32.5-percent-span station, while the results of reference 3 show that the boundary layer tended to collect at the 50-percent-span station. A schematic diagram of the boundary-layer thickness distribution of both tests is shown in figure 15. The difference in the boundary-layer formation is due to the difference in aspect ratio (from 0.378 to 1.00) and can be explained by the same line of reasoning presented in reference 3.

Figure 16 shows the stagnation-pressure-recovery distribution for the three spanwise stations as measured by the wake survey made at 0.66-chord length behind the trailing edges of the blades (see fig. 7) and also the location of the centers of maximum wake depressions with respect to the trailing edges of the blades. If the wake centers can be used as an indication of the direction of the streamlines of the flow leaving the blades, then the displacement of these centers from lines drawn from the trailing edges of the blades, representing the streamlines for a 90° turn, indicates the amount of deviation from a 90° turn. It can be seen from figure 16 that a turn very close to 90° was obtained at the 10-percent-span and the 50-percent-span stations whereas a turn of less than 90° was obtained at the 32.5-percent-span station. The average turning angle, however, was within about 1° of design. The variation of the turning angle is attributed to the variation of the boundary-layer thickness across the span on the convex surface (see fig. 15).

Figure 17 is a shadowgraph of the flow. The passage at the top has more disturbances than the lower two because a shock wave from the nozzle enters the passage. The flow pattern at the entrance of the passages (see center passage, fig. 17) does not follow closely the theoretical characteristics calculations (fig. 1). This can be attributed to the entrance Mach number, which is higher than the design Mach number. However, the flow just ahead of the exit has only minor discontinuities. The disturbances from the trailing edge of the blade are due to the boundary layer on the blade. The shadowgraph shows that a disturbance exists at the surface of the uppermost external passage where the passage ends and the spacer starts. The disturbance is due to a slight misalinement of the flat surface of the spacer with the curved surface of the passage.

This disturbance appears to decrease in intensity as it moves away from the wall and becomes weak in the zone of the wake of the lower blade. Because no appreciable difference existed between the wake-survey results in the zone of the two blades, the effect of this disturbance must be small. The effect of the disturbance will be a small decrease in turning angle and an increase in mixing losses.

The stagnation-pressure recovery obtained from the average of the three stations for the survey inside the passage is 0.96. Theoretical calculations indicate a loss of about 0.02 due to the shocks in the passage. The other losses are due to the boundary layer. The stagnation-pressure recovery obtained from the average of the three stations of the wake survey is 0.91. This shows a loss in stagnation-pressure recovery of 0.05 due to the mixing process.

CONCLUSIONS

The tests of a two-dimensional cascade of three 90° turning passages at an inlet Mach number of 1.81 indicate the following:

1. Although a variation of the boundary-layer thickness occurred across the span and resulted in a nonuniform turning angle, the average turning angle was within 1° of the design value.

2. The total loss in stagnation across the cascade was 9 percent. Of this total, approximately 5 percent is chargeable to the mixing process downstream of the trailing edges.

3. The wake survey indicates that the velocity tends to become uniform very rapidly behind the trailing edge in the blade wake.

Langley Aeronautical Laboratory
National Advisory Committee for Aeronautics
Langley Air Force Base, Va.

APPENDIX

METHOD OF CALCULATION

The local values of Mach number were obtained from the measured static pressure and the pressure indicated by a pitot tube. The stagnation pressure was then determined from the Mach number and the pitot-tube pressures. The Mach number and the stagnation pressure were used to calculate the average Mach number and the average stagnation pressure. The average weighted stagnation pressure and the average weighted Mach number were computed and are given by the following expressions:

$$P_{2_{av}} = \frac{1}{m} \int_{A_2} P_2 \, dm$$

$$\frac{P_{2_{av}}}{P_o} = \frac{\int_{A_2} \left(M_2 \frac{P_2}{P_o} \frac{p_2}{p_o} \sqrt{\frac{T_o}{T_2}} \right) ds}{\int_{A_2} \left(M_2 \frac{p_2}{p_2} \sqrt{\frac{T_o}{T_2}} \right) ds}$$

$$M_{2_{av}} = \frac{1}{m} \int_{A_2} M_2 \, dm$$

$$\frac{M_{2_{av}}}{M_1} = \frac{\int_{A_2} \left(M_2 \frac{M_2}{M_1} \frac{p_2}{p_o} \sqrt{\frac{T_o}{T_2}} \right) ds}{\int_{A_2} \left(M_2 \frac{p_2}{p_o} \sqrt{\frac{T_o}{T_2}} \right) ds}$$

For the results presented, the mass flow measured at each span station was considered as a third of the total mass flow.

[redacted]

REFERENCES

1. Kantrowitz, Arthur: The Supersonic Axial-Flow Compressor. NACA Rep. 974, 1950.

2. Ferri, Antonio: Preliminary Analysis of Axial-Flow Compressors Having Supersonic Velocity at the Entrance of the Stator. NACA RM L9G06, 1949.

3. Liccini, Luke L.: Analytical and Experimental Investigation of 90° Supersonic Turning Passages Suitable for Supersonic Compressors or Turbines. NACA RM L9G07, 1949.

[redacted]

TABLE I

BLADE CHARACTERISTICS OF MODEL 3 OF REFERENCE 3

AND BLADE OF PRESENT TEST

Parameters	Model 3 of reference 3	Blade of present test
Chord, inches	5.3	3.0
Span, inches	2.0	3.0
Thickness ratio, t/c, percent . .	12.26	12.26
Solidity, c/s	3.12	3.12
Aspect ratio	0.378	1.00

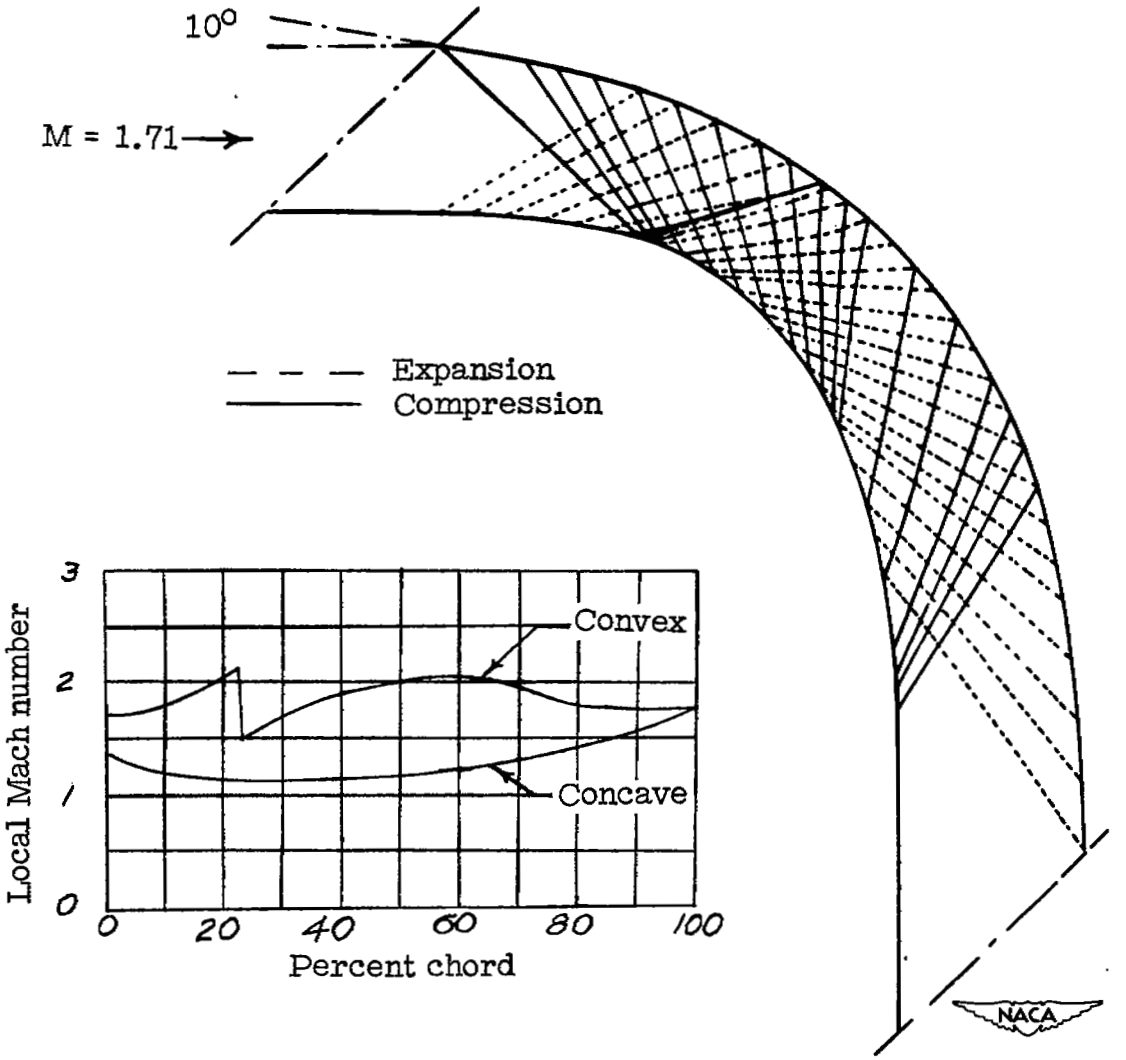

Figure 1.- Characteristics net and the variation of local Mach number with percent chord.

Station	Ordinates (percent chord) Upper surface	Lower surface
0	0	0
5	5.60	3.71
10	10.45	7.08
20	20.65	12.74
30	27.04	16.66
40	30.50	19.13
50	30.94	19.81
60	28.77	19.20
70	24.29	16.98
80	18.02	13.05
90	9.79	7.31
100	0	0

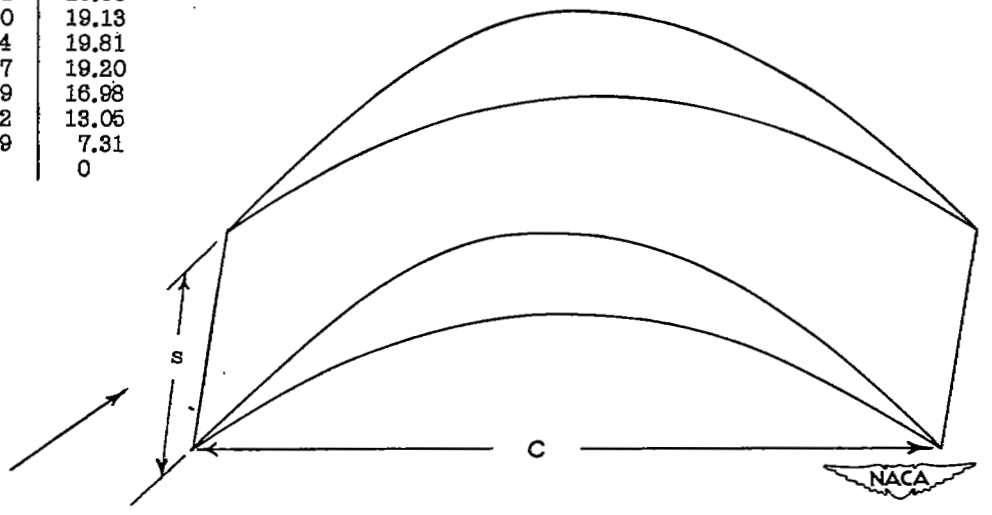

Figure 2.- Blade shape and corresponding ordinates.

[redacted]

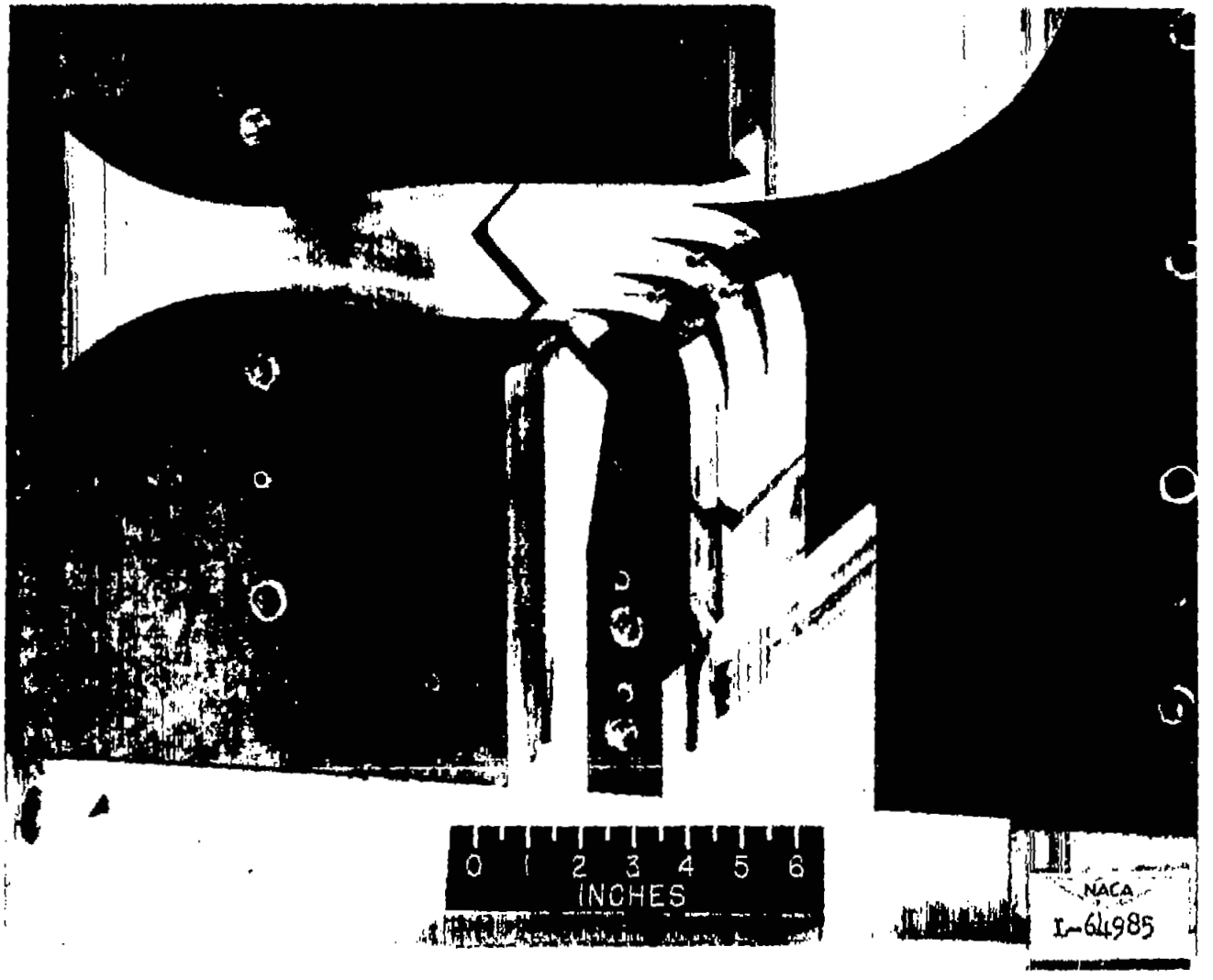

Figure 3.- Photograph of cascade assembly in test setup with one side wall removed.

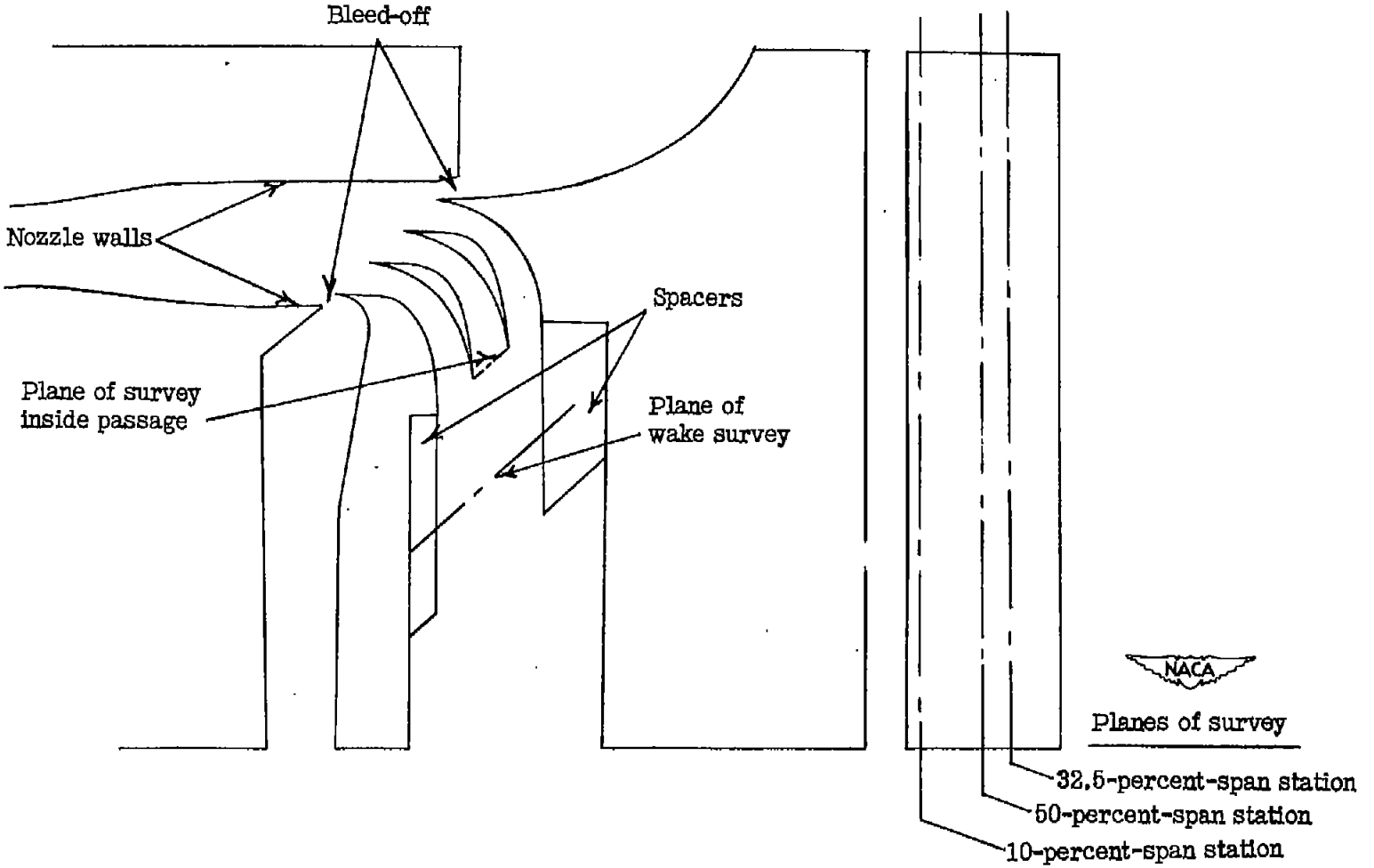

Figure 4.- Schematic diagram of test setup.

NACA
L-64988

Figure 5.- Photograph of the blade.

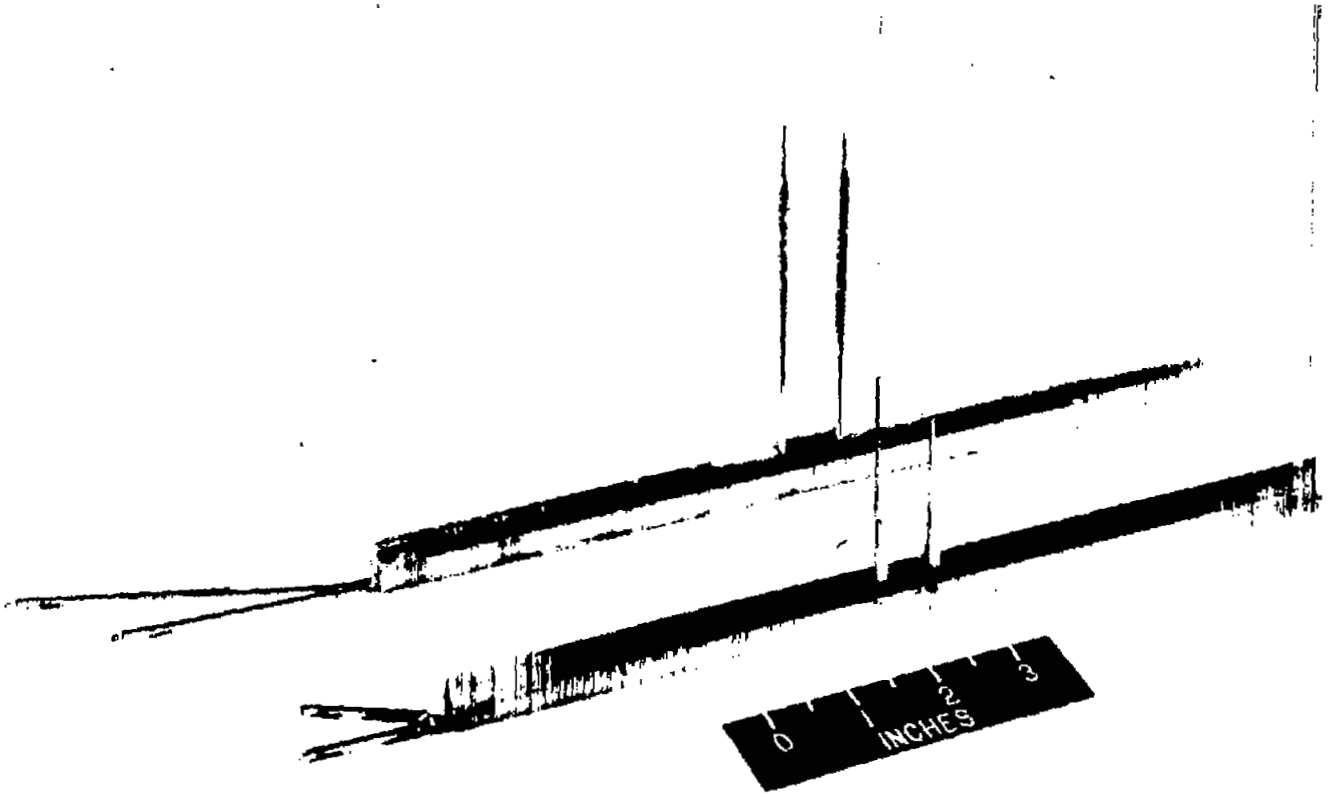

Figure 6.- Photograph of the rakes.

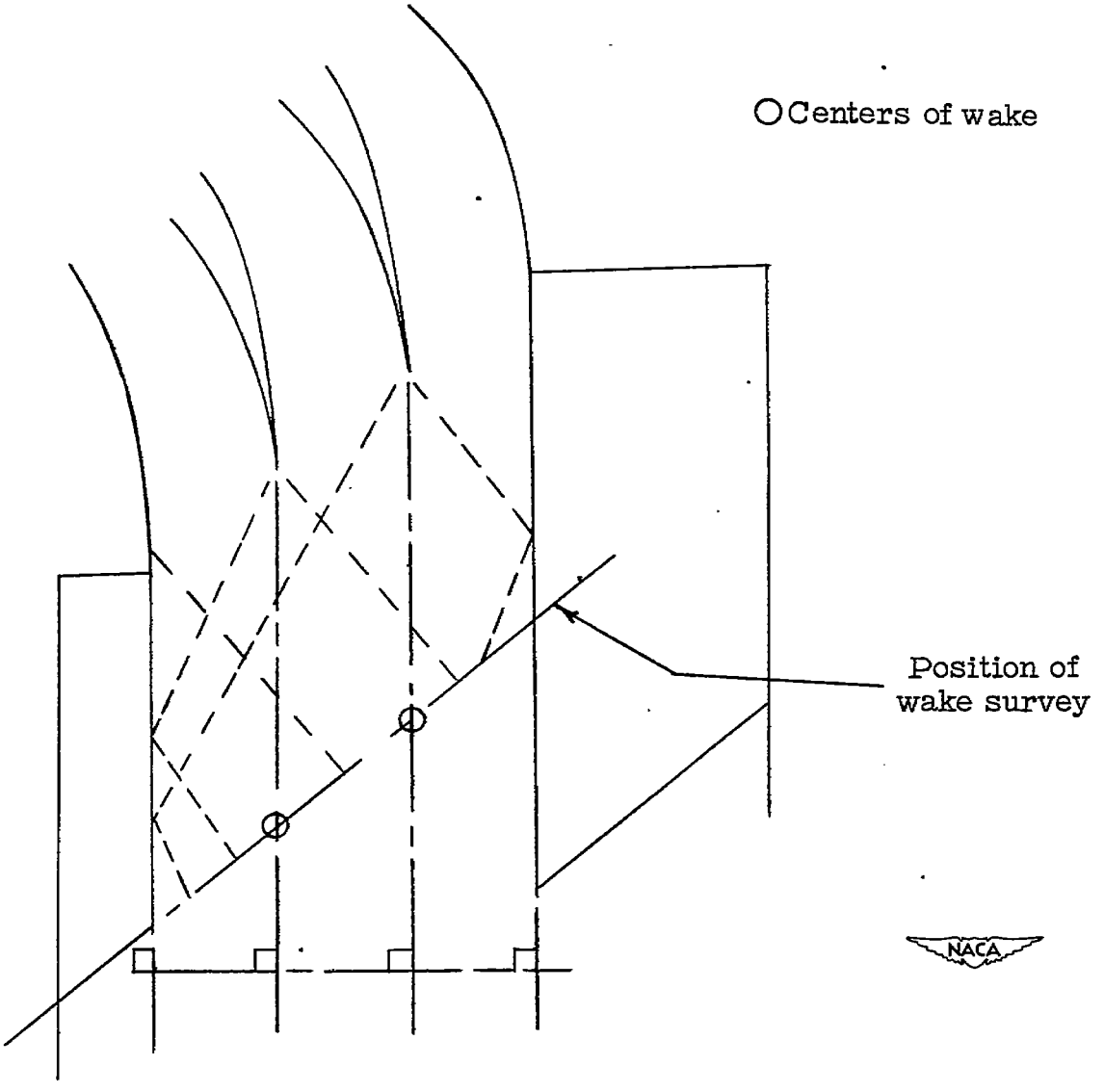

Figure 7.- Schematic diagram of the flow disturbances behind the exit of the cascade as obtained from the shadowgraph.

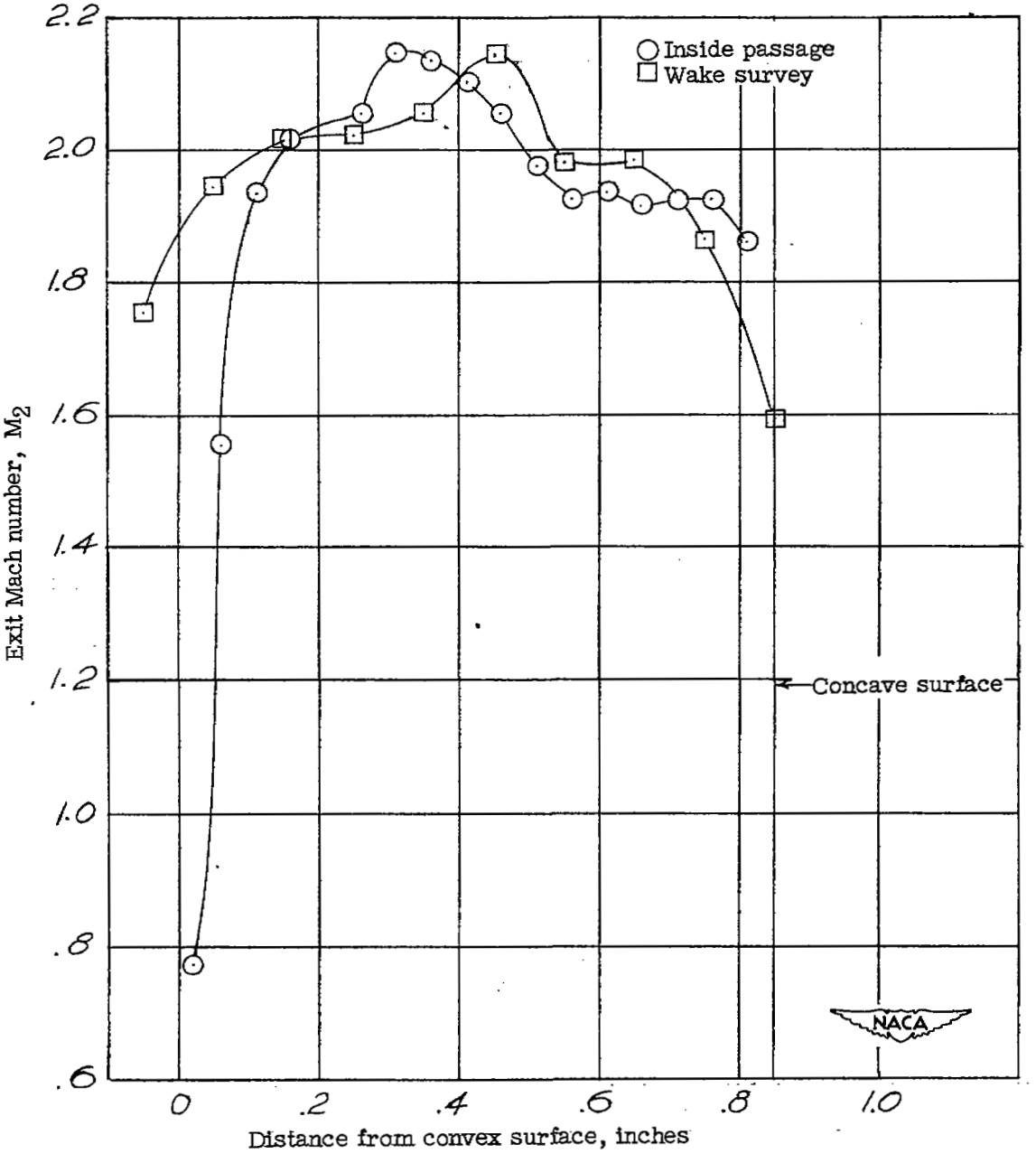

Figure 8.- The variation of the exit Mach number inside the exit of the passage and the corresponding zone of the wake survey with distance from convex surface at the 50-percent-span station.

[redacted]

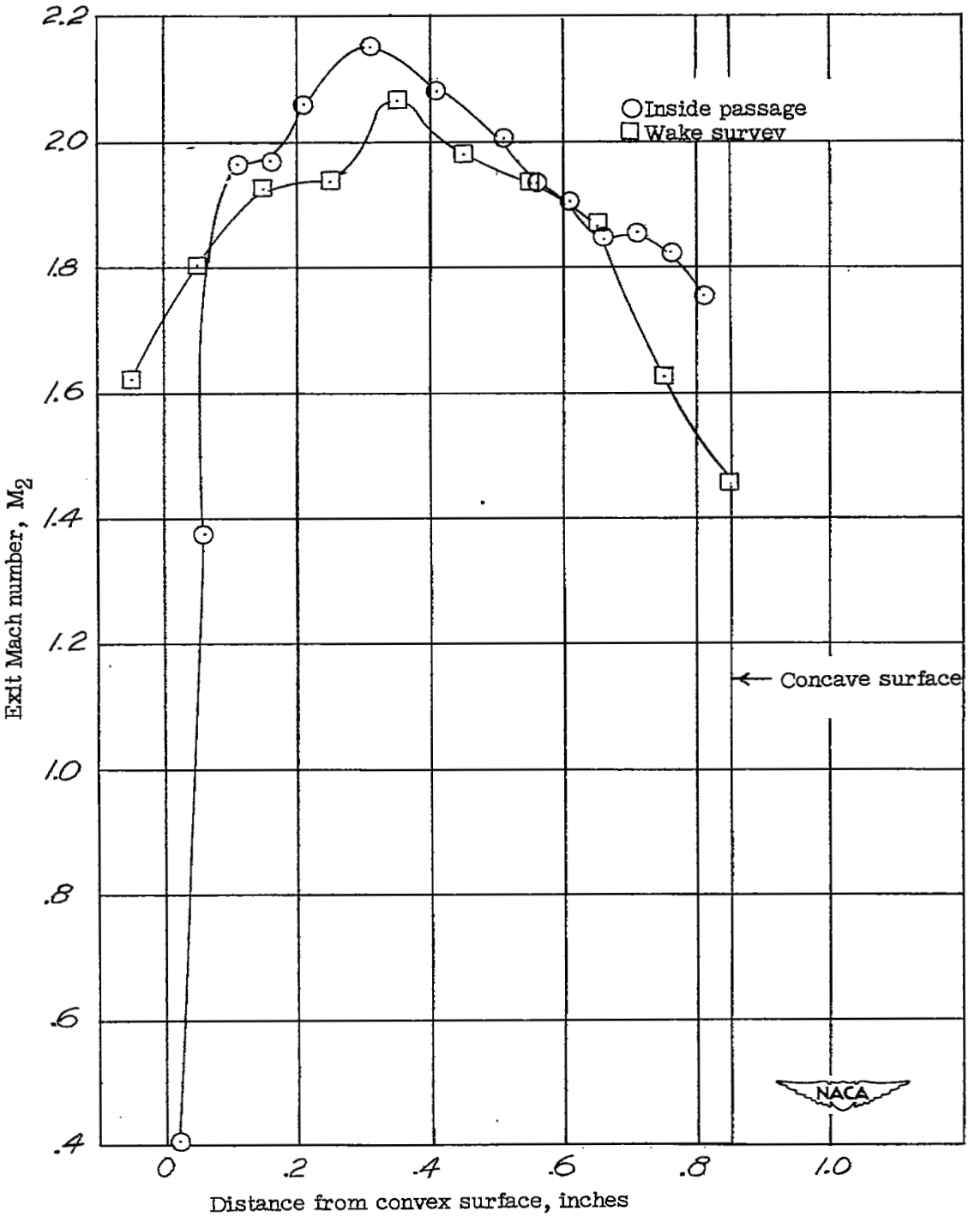

Figure 9.- The variation of the exit Mach number inside the exit of the passage and the corresponding zone of the wake survey with distance from convex surface at the 32.5-percent-span station.

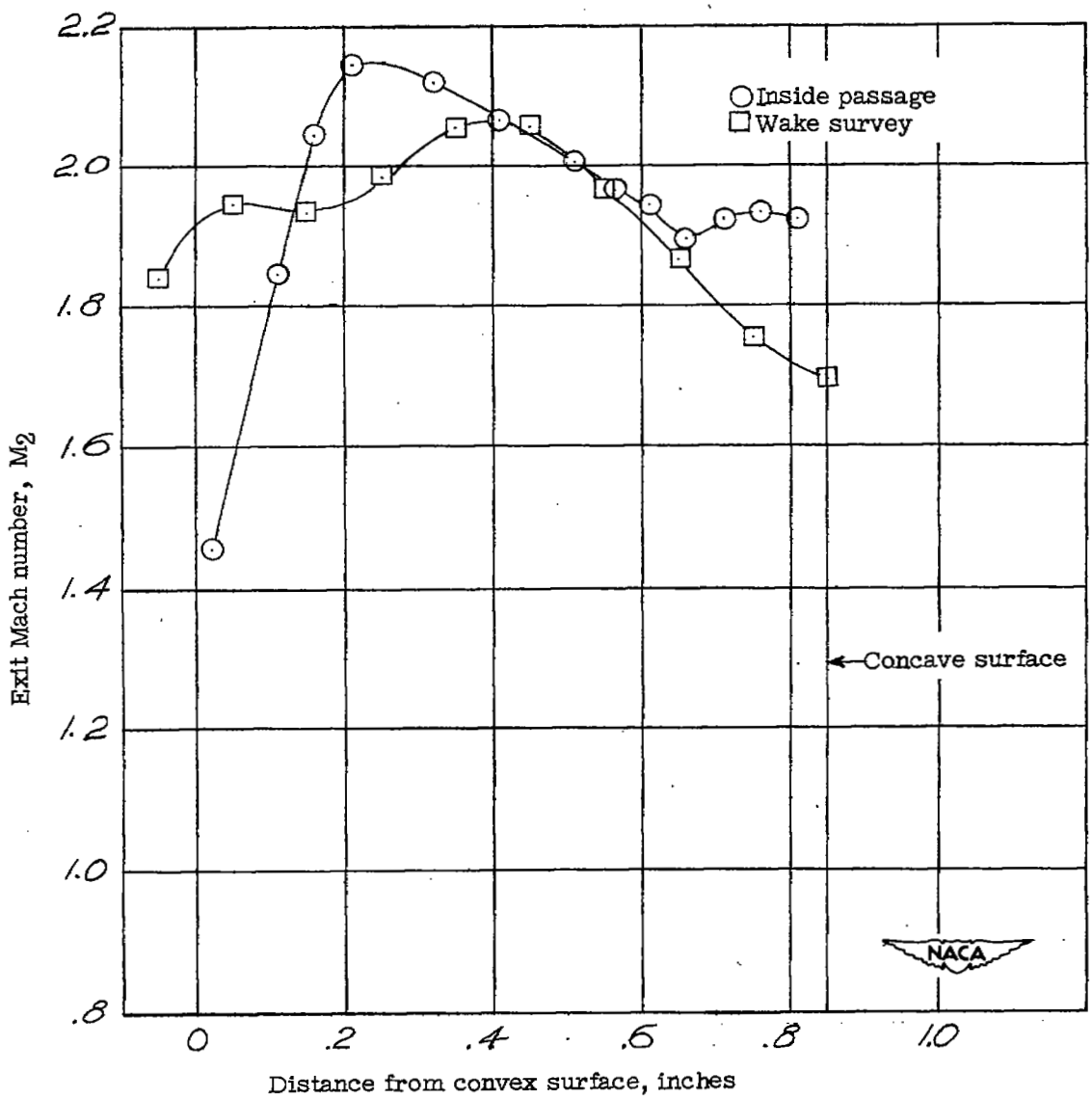

Figure 10.- The variation of the exit Mach number inside the exit of the passage and the corresponding zone of the wake survey with distance from convex surface at the 10-percent-span station.

[redacted]

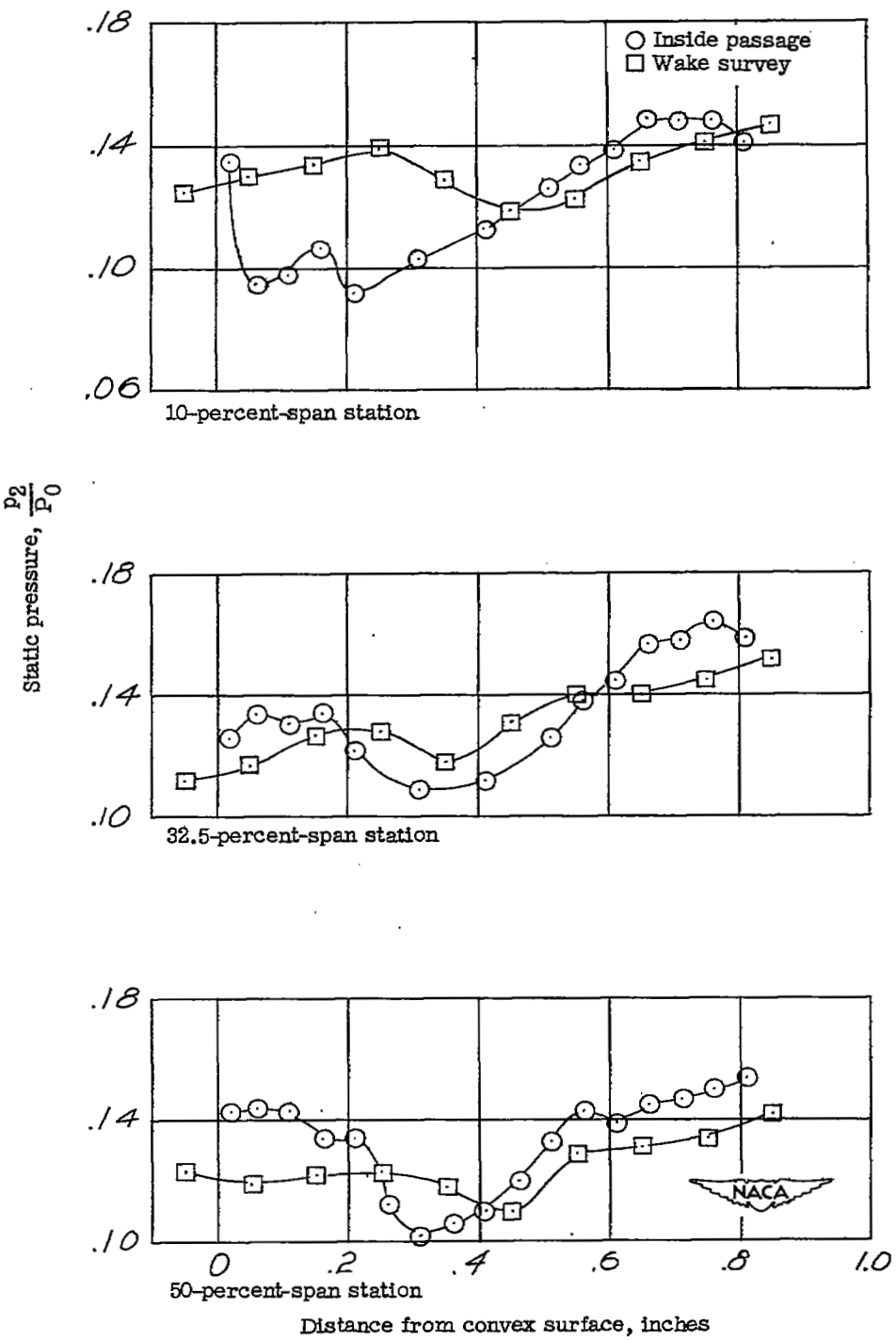

Figure 11.- Comparison of static-pressure distribution at the three spanwise stations for the survey inside the passage with the corresponding zones of the wake survey.

[redacted]

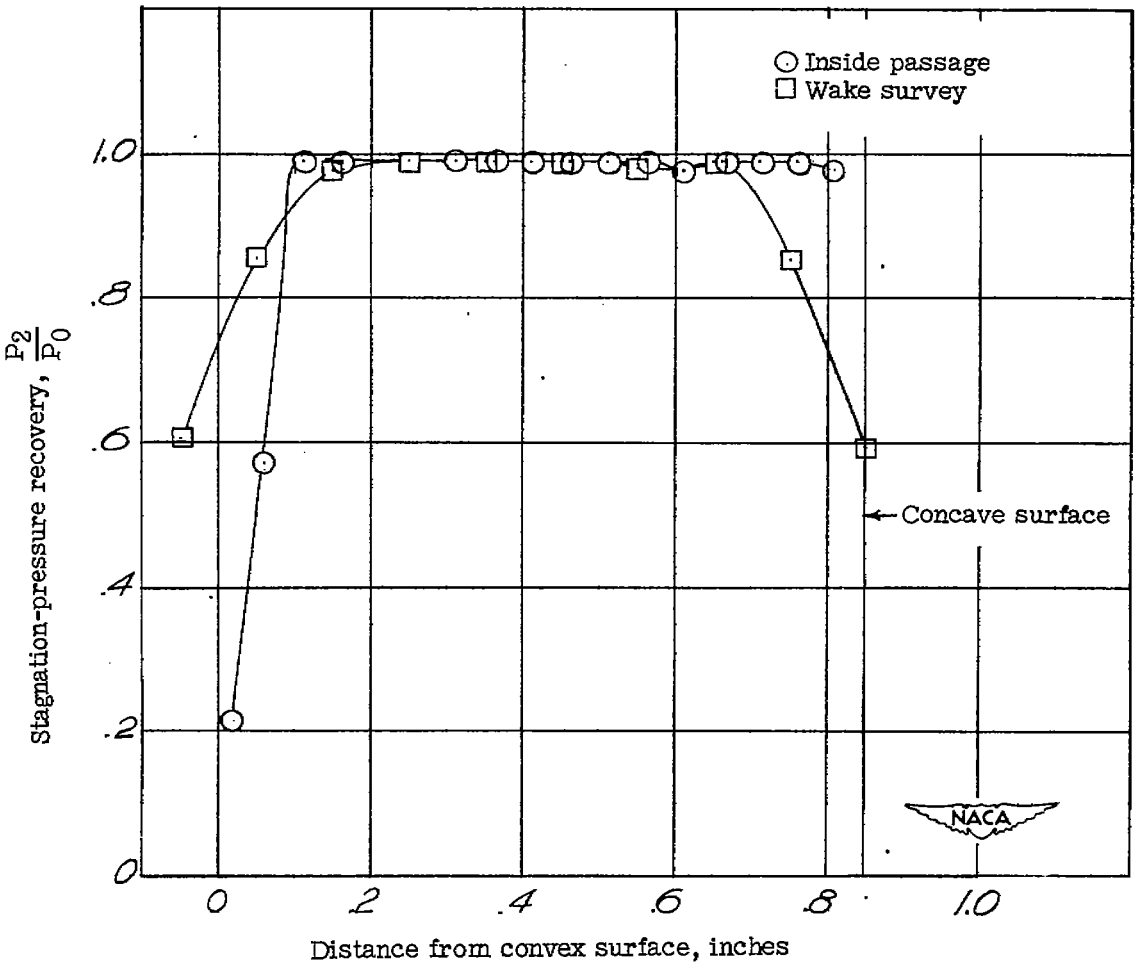

Figure 12.- The variation of stagnation-pressure recovery inside the exit of the passage and the corresponding zone of the wake survey with distance from convex surface at the 50-percent-span station.

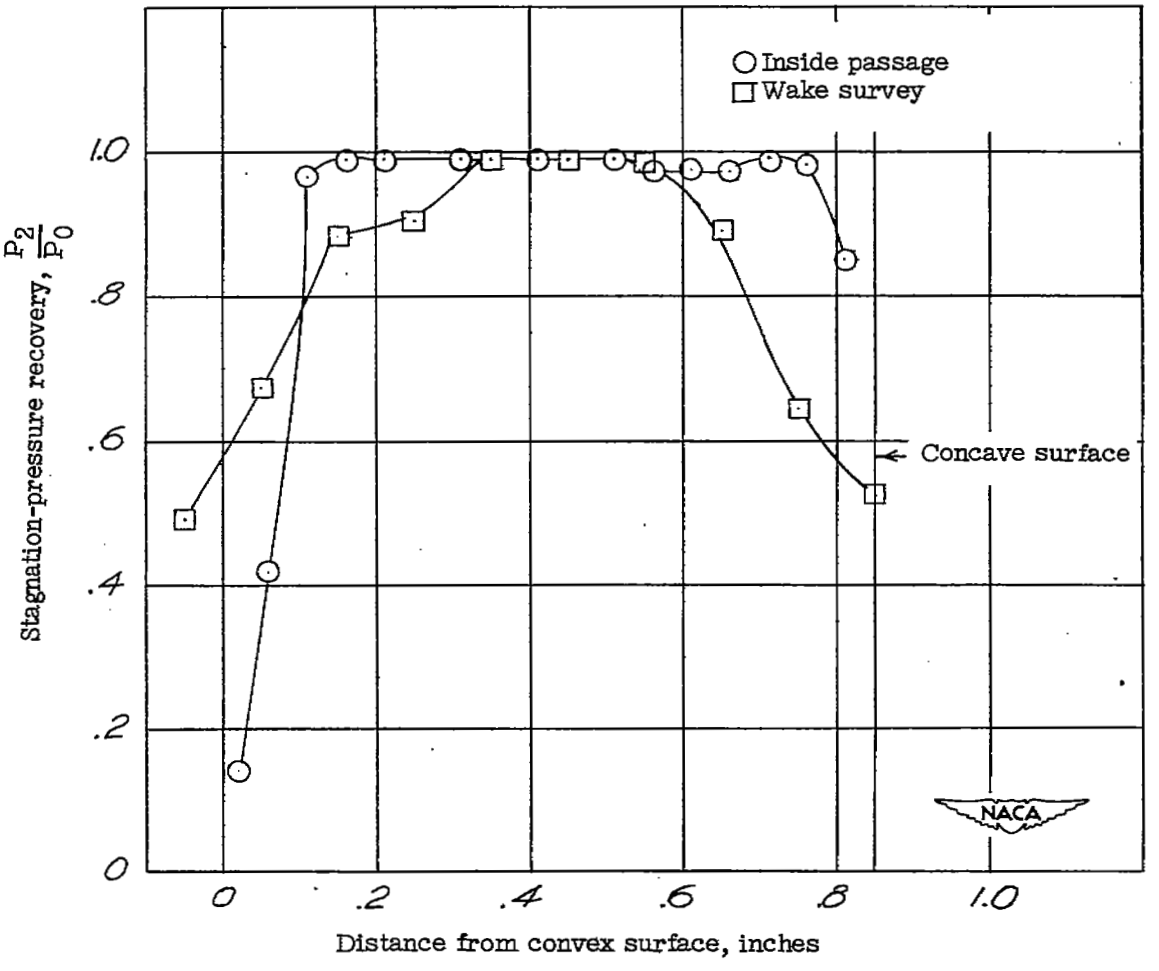

Figure 13.- The variation of stagnation-pressure recovery inside the exit of the passage and the corresponding zone of the wake survey with distance from convex surface at the 32.5-percent-span station.

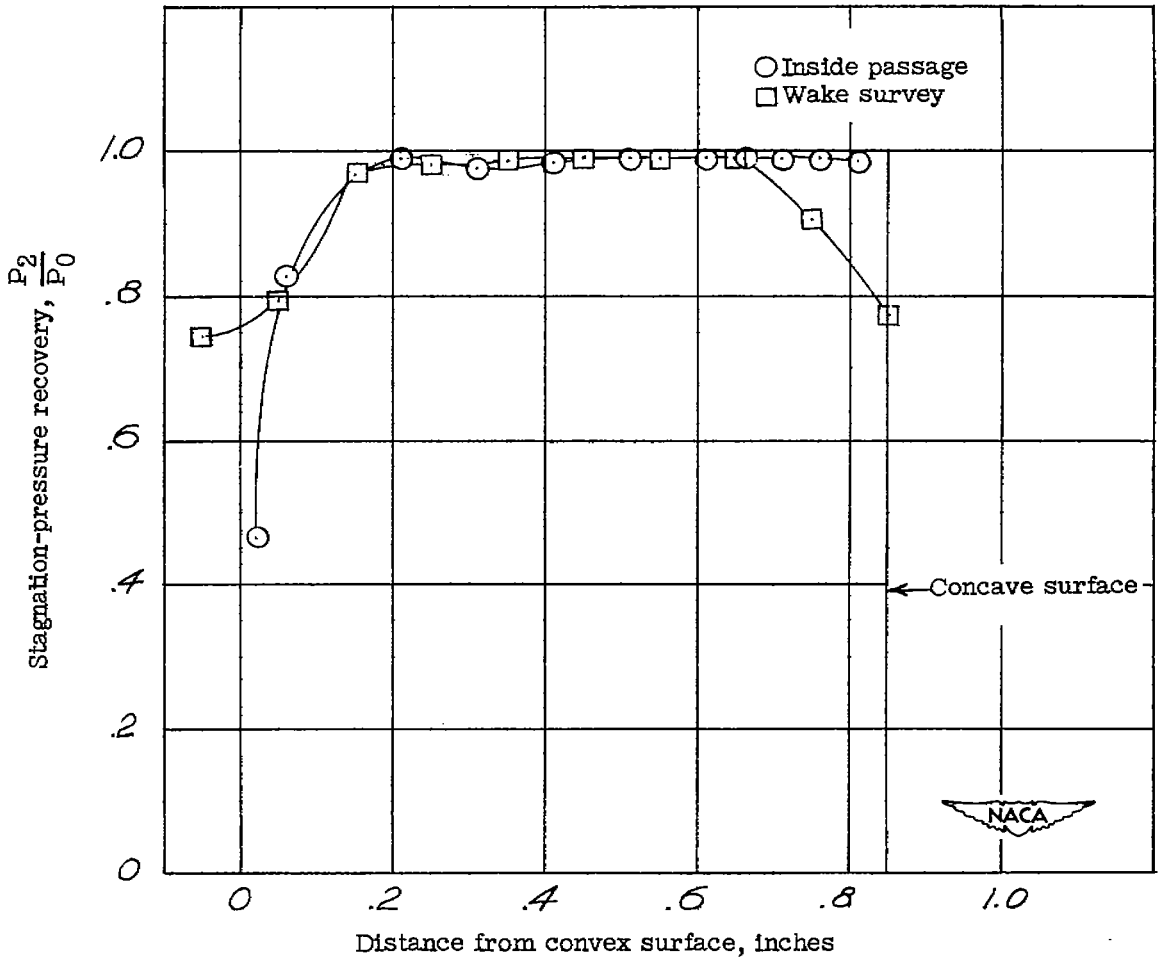

Figure 14.- The variation of stagnation-pressure recovery inside the exit of the passage and the corresponding zone of the wake survey with distance from convex surface at the 10-percent-span station.

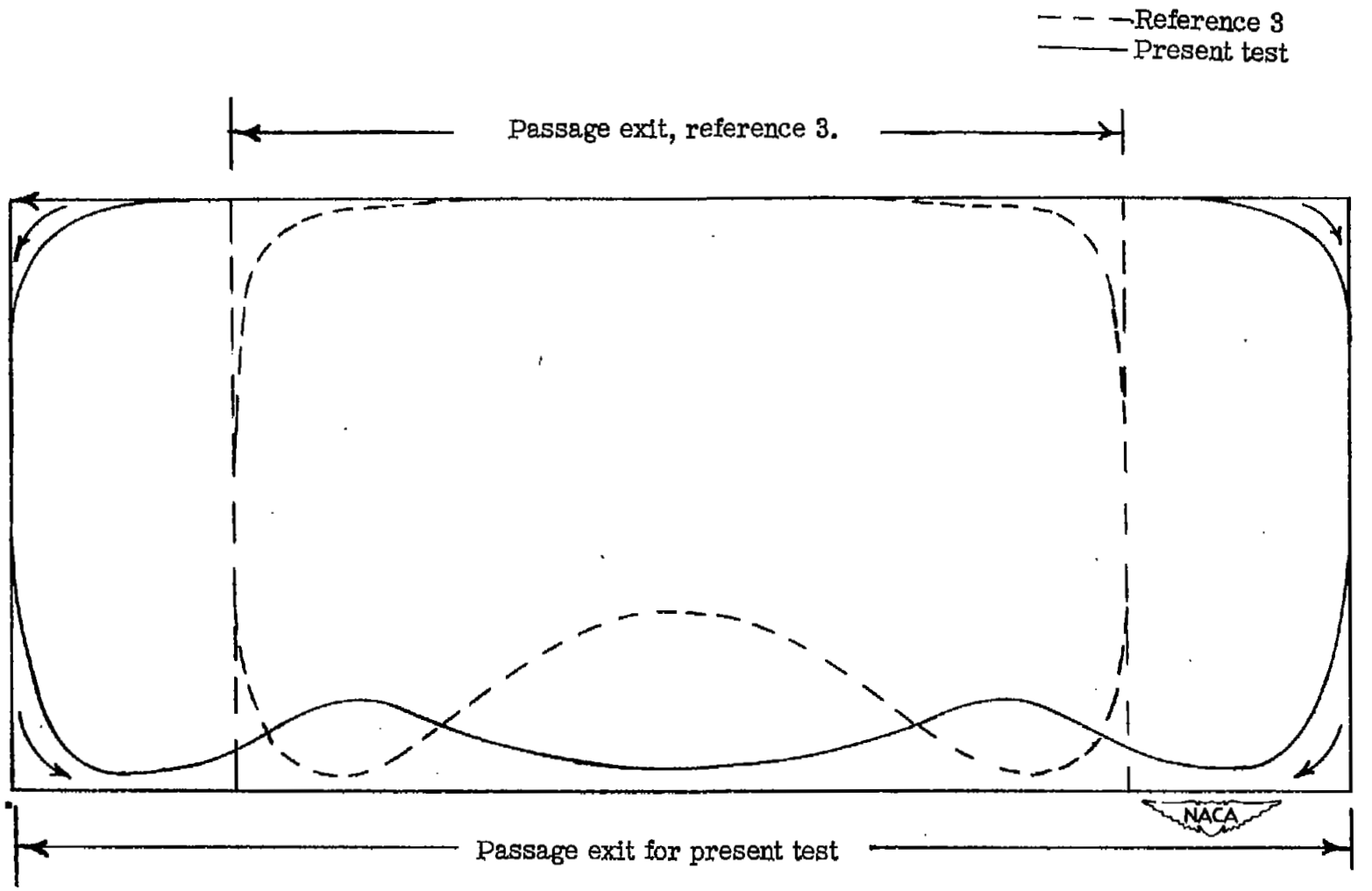

Figure 15.- Schematic diagram of the boundary-layer thickness compared to reference 3.

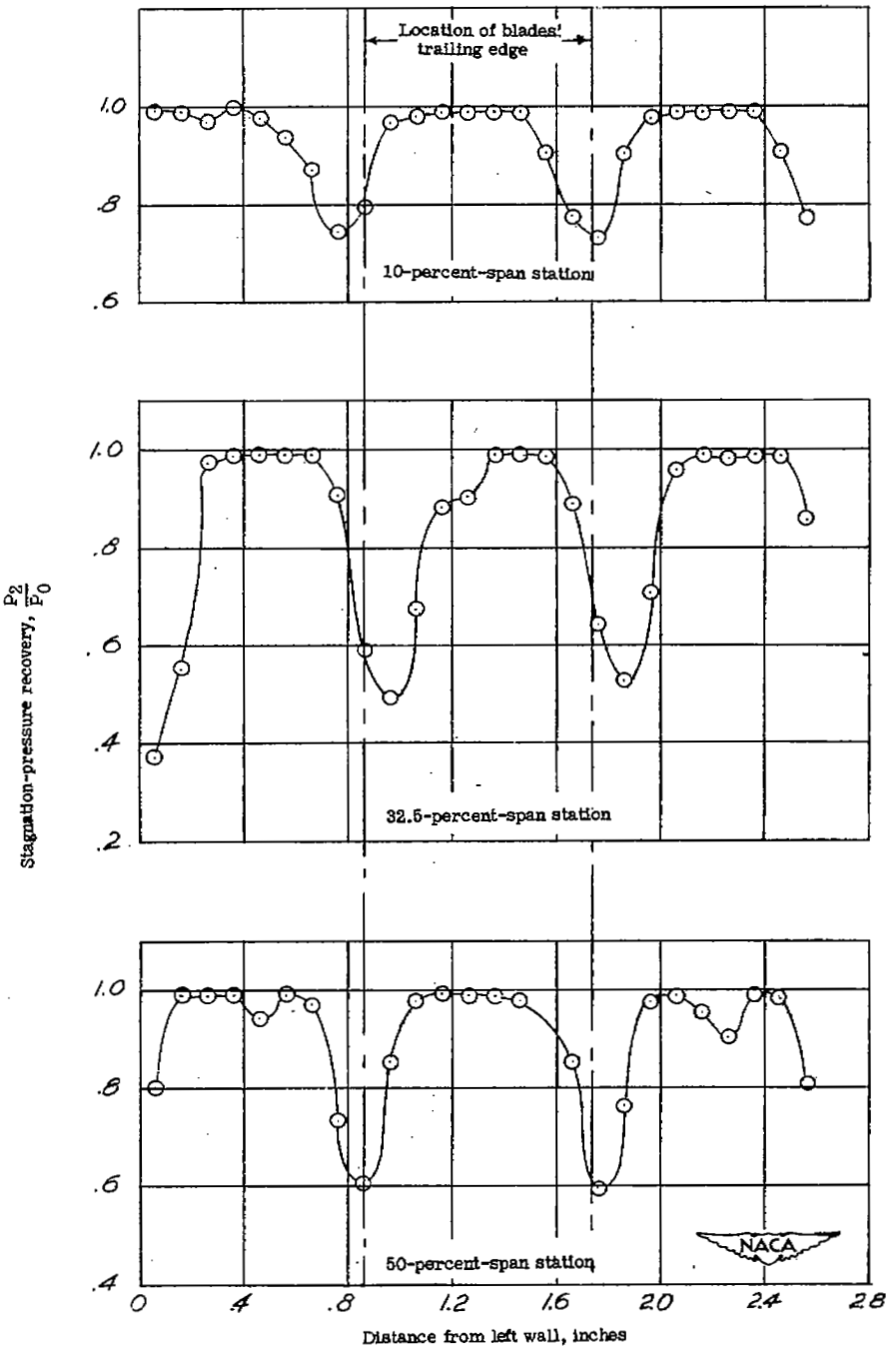

Figure 16.- Variation of stagnation-pressure recovery through the wake survey for three positions.

[redacted]

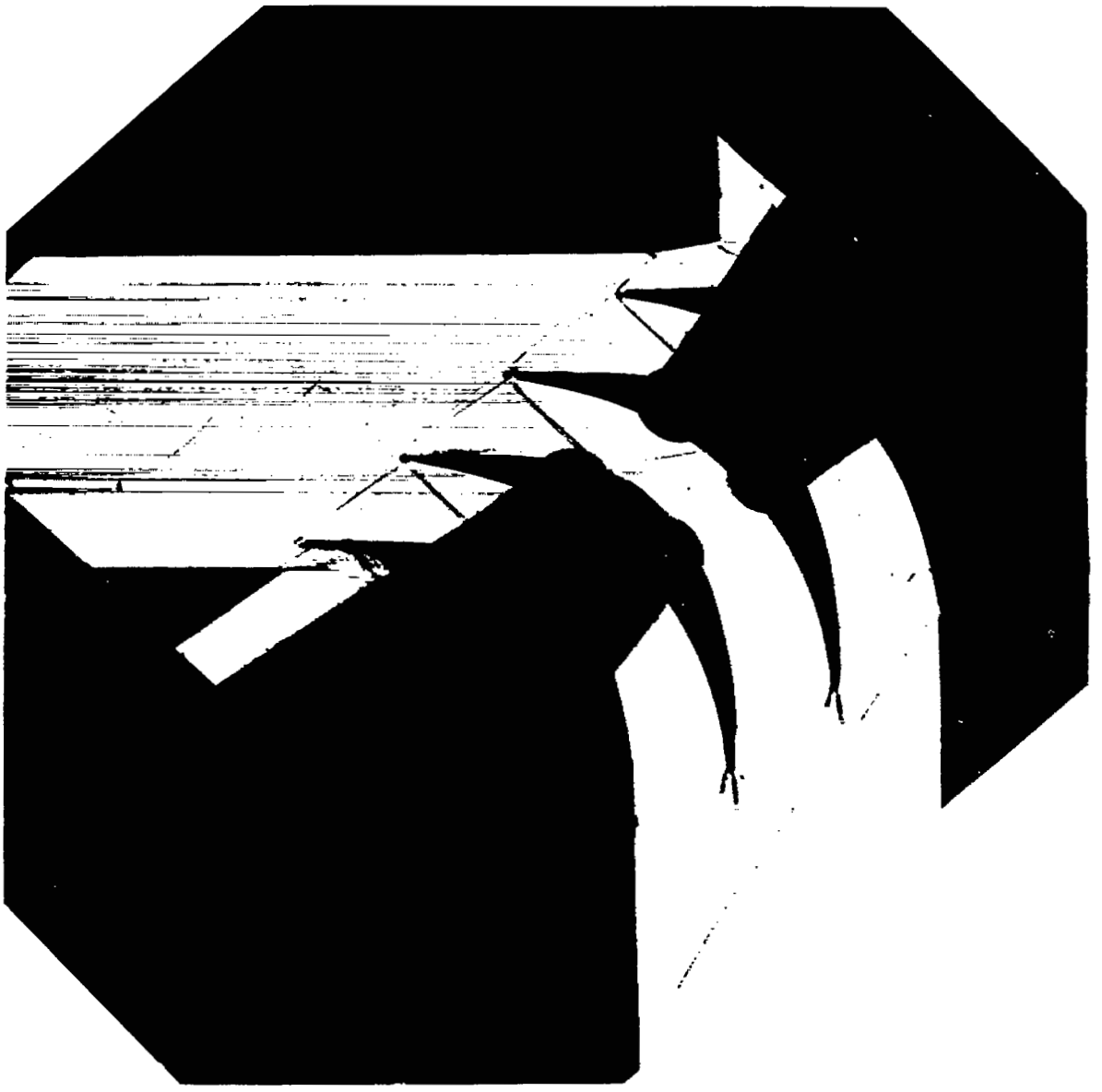

NACA
L-64903

Figure 17.- Shadowgraph of the flow in the cascade.

NACA-Langley - 8-15-50 -275